Article

Coded Amino Acids in Gas Phase: The Shape of Isoleucine

Alberto Lesarri, Raquel Snchez, Emilio J. Cocinero, Juan C. Lpez, and Jos L. Alonso

J. Am. Chem. Soc., **2005**, 127 (37), 12952-12956• DOI: 10.1021/ja0528073 • Publication Date (Web): 23 August 2005

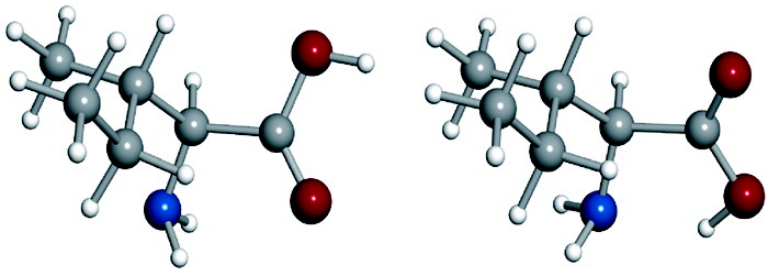

More About This Article

Additional resources and features associated with this article are available within the HTML version:

- Supporting Information
- Links to the 7 articles that cite this article, as of the time of this article download
- Access to high resolution figures
- Links to articles and content related to this article
- Copyright permission to reproduce figures and/or text from this article

View the Full Text HTML

J|A|C|S
ARTICLES
Published on Web 08/23/2005

Coded Amino Acids in Gas Phase: The Shape of Isoleucine

Alberto Lesarri, Raquel Sánchez, Emilio J. Cocinero, Juan C. López, and José L. Alonso*

Contribution from the Grupo de Espectroscopía Molecular (GEM), Departamento de Química Física y Química Inorgánica, Facultad de Ciencias, Universidad de Valladolid, 47005 Valladolid, Spain

Received April 29, 2005; E-mail: jlalonso@qf.uva.es

Abstract: The solid α-amino acid isoleucine has been vaporized by laser ablation and expanded in a supersonic jet, where the molecular conformations of the isolated molecule were probed using Fourier transform microwave spectroscopy. Two conformers of neutral isoleucine have been detected in gas phase, the most stable being stabilized by an intramolecular hydrogen bond N−H···O=C and a *cis*-COOH arrangement. The higher energy form is stabilized by an intramolecular hydrogen bond N···H−O. The *sec*-butyl side chain of the amino acid adopts the same configuration in the two observed conformers, with a staggered configuration at C_β similar to that observed in valine and a trans arrangement of C_α and C_δ. Ab initio calculations at MP2/6-311++G(d,p) level reproduce satisfactorily the experimental results.

Introduction

The dynamic role of α-amino acids ($NH_2-CH(R)-COOH$) as building blocks of proteins relies on their high torsional flexibility, which results in a large number of low energy conformational minima. The preferred conformations are determined by a delicate balance of different covalent and noncovalent interactions within the molecule and with its surroundings, especially hydrogen bonding. In particular, amino acids in crystals or solutions are stabilized as charge-separated zwitterions[1] ($NH_3^+-CH(R)-COO^-$) by a network of intermolecular hydrogen bond interactions. As a consequence, the intramolecular interactions and the intrinsic conformational preferences of these systems cannot be determined in condensed phases and are only revealed when the molecules are isolated in gas phase, where the amino acids exhibit an unsolvated neutral form ($NH_2-CH(R)-COOH$). This form represents the best approximation to the electronic environment of an amino acid residue in a polypeptide chain or protein. A supersonic jet expansion with an inert carrier gas is the preferred experimental approach to isolate the different conformers in their separated potential wells.[2] The strong collisional regime at the beginning of the adiabatic expansion produces a strong cooling of the rotational and vibrational states, and the individual conformers are usually frozen into the ground vibrational state of each individual well. In this way, the conformer distribution before the expansion may be preserved provided that interconversion barriers between conformers are sufficiently high. As the expansion evolves, the number of molecular collisions practically disappears, and thus the spectroscopic properties of the different species can be probed in a local environment of virtual isolation.

Different experimental methodologies have been used for the study in gas phase of amino acids and other small bioactive molecules.[3] Electronic spectroscopy of amino acids is limited to favorable cases that present aromatic chromophores.[4,5] The electronic spectrum of the different conformers can be analyzed with the aid of double resonance techniques (UV−UV,[6] IR−UV[7]) and ab initio theoretical predictions, but do not provide direct structural information since in most cases rotational resolution is not attainable. Rotational spectroscopy is the only technique that, thanks to its inherently superior resolution, can distinguish unambiguously between different isomers, conformers, or isotopomers and provide accurate structural information directly comparable to the in vacuo theoretical predictions. However, amino acids are difficult to vaporize since they are solids with high melting points and thermally unstable. For these reasons, most neutral amino acids have escaped for a long time to gas-phase spectroscopic investigation, and even the intrinsic conformational landscape of the genetically encoded amino acids is poorly known. The analysis of the rotational spectrum of natural amino acids, started in the late 1970s by Suenram and Godfrey on glycine[8,9] and later by Godfrey on alanine[10] and

(1) (a) Albrecht, G.; Corey, R. B. *J. Am. Chem. Soc.* **1939**, *61*, 1087. (b) Marsh, R. E. *Acta Crystallogr.* **1958**, *11*, 654. (c) Levy, H. A.; Corey, R. B. *J. Am. Chem. Soc.* **1941**, *63*, 2095. (d) Donohue, J. *J. Am. Chem. Soc.* **1950**, *72*, 949.
(2) (a) Levy, D. H. *Annu. Rev. Phys. Chem.* **1980**, *31*, 197. (b) *Jet Spectroscopy and Molecular Dynamics*; Hollas, J. M., Phillips, D., Eds.; Blackie: London, 1995.
(3) (a) Robertson, E. G.; Simons, J. P. *Phys. Chem. Chem. Phys.* **2001**, *3*, 1. (b) Weinkauf, R.; Schermann, J.-P.; de Vries, M. S.; Kleinermans, K. *Eur. Phys. J. D* **2002**, *20*, 309. (c) Zwier, S. *J. Phys. Chem. A* **2001**, *105*, 8827.
(4) Snoek, L. C.; Robertson, E. G.; Kroemer, R. T.; Simons, J. P. *Chem. Phys. Lett.* **2000**, *321*, 49.
(5) Bakker, J. M.; Aleese, L. M.; Meijer, G.; von Helden, G. *Phys. Rev. Lett.* **2003**, *91*, 203003.
(6) Lipert, R. J.; Colson, S. D. *Chem. Phys. Lett.* **1998**, *161*, 303.
(7) (a) Page, R. H.; Shen, Y. R.; Lee, Y. T. *J. Chem. Phys.* **1988**, *88*, 4621. (b) Page, R. H.; Shen, Y. R.; Lee, Y. T. *J. Chem. Phys.* **1988**, *88*, 5362.
(8) (a) Suenram, R. D.; Lovas, F. J. *J. Mol. Spectrosc.* **1978**, *72*, 372. (b) Suenram, R. D.; Lovas, F. J. *J. Am. Chem. Soc.* **1980**, *102*, 7180. (c) Lovas, F. J.; Kawashima, Y.; Grabow, J.-U.; Suenram, R. D.; Fraser, G. T.; Hirota, E. *Astrophys. J.* **1995**, *455*, L201.

10.1021/ja0528073 CCC: $30.25

Chart 1. Possible Configurations of the α-Amino Acid Backbone, Associated with Different Intramolecular Hydrogen Bonds

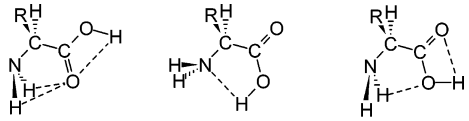

Configuration I Configuration II Configuration III

β-alanine,[11] was refrained for a long time by the difficulties to bring these compounds into gas phase. We have recently impulsed this field with the combination of laser ablation with Fourier transform microwave spectroscopy in supersonic jets[12] (laser-ablation molecular-beam FT-microwave spectroscopy, LA-MB-FTMW). In this experimental approach, the solid sample is vaporized with a short visible laser pulse. The vaporized molecules of the solid can then be seeded into an expanding stream of an inert carrier gas and probed using Fourier transform microwave spectroscopy.[13] To date, several natural amino acids (proline,[14] alanine,[15] valine,[16] 4(*R*)-hydroxyproline, and 4(*S*)-hydroxyproline[17]) and other organic solids such as thiourea[18] have been studied using LA-MB-FTMW.

Isoleucine (mp 295−300 °C) is an essential aliphatic α-amino acid not synthesized by mammalian tissues, characterized by a (2*S*,3*S*) *sec*-butyl side chain (R = $-CH(CH_3)CH_2CH_3$). Isoleucine is found mostly in the interior of proteins and enzymes helping to dictate the tertiary structure of a macromolecule, as in the hydrophobic core of vertebrate insulins.[19] There are no structural investigations of isoleucine in gas phase or any previous theoretical study. As occurs for smaller aliphatic amino acids such as glycine[8,9] (R = H), alanine[10,15] (R = CH_3), and valine[16] (R = $CH-(CH_3)_2$), the conformational behavior of isoleucine can be expected to be primarly governed by the intramolecular hydrogen bonding within the amino acid backbone, shown in Chart 1. The most stable configuration I is stabilized by an intramolecular amine-to-carbonyl (N−H···O═C) hydrogen bond and a *cis*-carboxylic functional group interaction, while configuration II exhibits an intramolecular hydrogen bond between the hydrogen atom of the hydroxyl group and the lone pair at the nitrogen atom (N···H−O). A third type of intramolecular hydrogen bond between the amino group and the oxygen atom of the carboxyl group (N−H···O−H) gives rise to configuration III, which has not been observed in the gas phase. The increase of the size of the side chain in isoleucine compared to those of alanine or valine complicates considerably the conformational landscape of the molecule, resulting in a greater number of plausible conformers. The present experimental observations of isoleucine by our LA-MB-FTMW technique will provide unique experimental information on the structures of the individual conformers of this coded amino acid, contributing to improve our understanding of the role of intramolecular forces in the conformational behavior of amino acids in the gas phase.

Experimental and Theoretical Methods

1. Laser Ablation and Rotational Spectroscopy. The LA-MB-FTMW spectrometer and the experimental procedure have been described in detail elsewhere.[12] Solid isoleucine (mp 288 °C) was obtained commercially, pulverized, and pressed with minimum quantities of a binder (1−3 drops/g) to form cylindrical target rods of 6-mm diameter and 1−2-cm long. The targets are accommodated on a special pulsed injection nozzle located on the backside of one of the mirrors forming the Fabry−Pérot resonator, where they are vaporized with the 532-nm green pulses (∼10 ns) of a doubled Q-switched Nd:YAG laser focused to give irradiances ca. 10^8 W cm^{-2}. The whole injection system is removable and can be extracted from the backside of the Fabry−Pérot mirror through an auxiliary chamber to facilitate replacing of the sample. The injection system and the microwave resonator are housed in a high vacuum tank evacuated to 10^{-6} mbar prior to expansion. In each operation cycle the ablation products are seeded in a carrier gas flow and expanded supersonically in the region along the axis of the Fabry−Pérot microwave resonator where they are probed using Fourier transform microwave spectroscopy in the region 6−18 GHz. In this work, neon at stagnation pressures ca. 5 bar was used as the carrier gas with nozzle openings of 0.5−0.7 ms. Microwave pulses of 0.2−0.4 μs (1−30 mW) applied to the center of the resonator through a coaxial antenna polarizes the molecules in the jet. Finally, the microwave transient free-induction decay associated to molecular relaxation is down-converted and registered in the time domain at 40−100-ns intervals. A Fourier transformation yields the resonant frequencies of the rotational transitions with a maximum resolution of ca. 3 kHz. The coaxial arrangement of the supersonic jet and the axis of the resonator produces a Doppler doubling of the observed transitions, and thus the rest frequencies are calculated as the arithmetic mean of the two Doppler components. The accuracy of the frequency measurements is better than 3 kHz.

2. Ab Initio Calculations. Theoretical predictions have been used to locate the most stable conformers on the potential energy surface and to calculate the molecular properties relevant for the analysis of the rotational spectrum, such as rotational constants, electric dipole moments, and ^{14}N nuclear quadrupole coupling constants. A large number of conformers are conceivable by considering the possible rotations around all single bonds of the molecule. Our procedure for locating starting geometries was based on identifying plausible intramolecular interactions. The three configurations of Chart 1 resulting from the three intramolecular hydrogen bonds between the amino and carboxylic moieties were first considered and labeled with the convention used in lower aliphatic amino acids as configuration I (N−H···O═C, *cis*-COOH), II (N···H−O, *trans*-COOH), and III (N−H···O−H, *cis*-COOH). Next, the plausible orientations of the *sec*-butyl side chain were examined. Rotation about the $C_\alpha-C_\beta$ bond generates the three unstrained staggered configurations of Chart 2, labeled analogously to valine[16] as "a" ($\angle(H_\alpha-C_\alpha-C_\beta-H_\beta) \approx 60°$), "b" ($\angle(H_\alpha-C_\alpha-C_\beta-H_\beta) \approx 180°$), and "c" ($\angle(H_\alpha-C_\alpha-C_\beta-H_\beta) \approx 300°$). Finally, the presence of an additional methyl group 3-fold rotor at C_γ gives rise to three staggered alternatives shown in Chart 3 for each of the above configurations which have been labeled using additional subscripts as "1" ($\angle(C_\alpha-C_\beta-C_\gamma-C_\delta) \approx 180°$), "2" ($\angle(C_\alpha-C_\beta-C_\gamma-C_\delta) \approx 300°$), and "3" ($\angle(C_\alpha-C_\beta-C_\gamma-C_\delta) \approx 60°$). In this way, a total of 3 × 3 ×

(9) (a) Brown, R. D.; Godfrey, P. D.; Storey, J. W. V.; Bassez, M. P. *J. Chem. Soc., Chem. Commun.* **1978**, *547*. (b) Godfrey, P. D.; Brown, R. D. *J. Am. Chem. Soc.* **1995**, *117*, 2019. (c) McGlone, S. J.; Elmes, P. S.; Brown, R. D.; Godfrey, P. D. *J. Mol. Struct.* **1999**, *485*, 225.
(10) Godfrey, P. D.; Firth, S.; Hatherley, L. D.; Brown, R. D.; Pierlot, A. P. *J. Am. Chem. Soc.* **1993**, *115*, 9687.
(11) McGlone, S. J.; Godfrey, P. D. *J. Am. Chem. Soc.* **1993**, *117*, 1043.
(12) Lesarri, A.; Mata, S.; López, J. C.; Alonso, J. L. *Rev. Sci. Instrum.* **2003**, *74*, 4799.
(13) (a) Balle, T. J.; Flygare, W. H. *Rev. Sci. Instrum.* **1981**, *52*, 33. (b) Alonso, J. L.; Lorenzo, F. J.; Lopez, J. C.; Lesarri, A.; Mata, S.; Dreizler, H. *Chem. Phys.* **1997**, *218*, 267.
(14) Lesarri, A.; Mata, S.; Cocinero, E. J.; Blanco, S.; López, J. C.; Alonso, J. L. *Angew. Chem., Int. Ed.* **2002**, *41*, 4673.
(15) Blanco, S.; Lesarri, A.; López, J. C.; Alonso, J. L. *J. Am. Chem. Soc.* **2004**, *126*, 11675.
(16) Lesarri, A.; Cocinero, E. J.; López, J. C.; Alonso, J. L. *Angew. Chem., Int. Ed.* **2004**, *43*, 605.
(17) Lesarri, A.; Cocinero, E. J.; López, J. C.; Alonso, J. L. *J. Am. Chem. Soc.* **2005**, *127*, 2572.
(18) Lesarri, A.; Mata, S.; Blanco, S.; López, J. C.; Alonso J. L. *J. Chem. Phys.* **2004**, *120*, 6191.
(19) Baker, E. N.; Blundell, T. L.; Cutfield, J. F.; Cutfield, S. M.; Dodson, E. J.; Dodson G. G.; Crowfoot Hodgkin, D. M.; Hubbard, R. E.; Isaacs, N. W.; Reynolds, C. D.; Sakabe, K.; Sakabe, N.; Vijayan, N. M. *Philos. Trans. R. Soc. London* **1988**, *319*, 369.

Chart 2. Possible Configurations Associated with Rotation around the $C_\alpha - C_\beta$ Bond

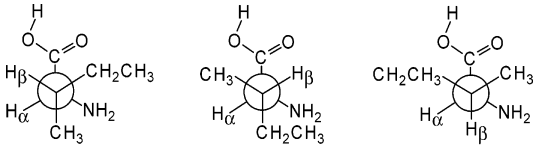

Chart 3. Possible Configurations Associated with Rotation around the $C_\beta - C_\gamma$ Bond

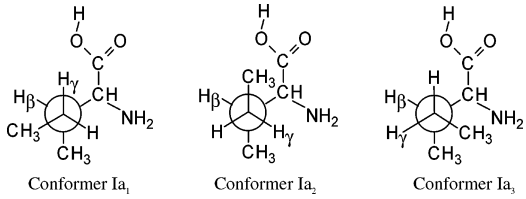

3 = 27 starting configurations were considered for isoleucine. Initial calculations used a computationally effective B3LYP density functional model with a standard 6-311++G(d,p) basis set and provided a first energy ordering of the conformers. In a second step, the 10 lowest energy structures shown in Figure 1 were submitted to a full energy optimization using second-order Møller−Plesset perturbation theory in the frozen core approximation with the same basis set.[20] This level of theory behaved satisfactorily in previous studies of amino acids.[15−17] The calculated equilibrium rotational constants, electric dipole moment components, and nuclear quadrupole coupling constants are presented in Table 1. Since the lowest energy conformers appeared to be close in energy, the calculation of relative stabilities was improved, including the zero-point vibrational contributions, derived using the B3LYP functional in the harmonic approximation. The predicted global minimum is the Ia_1 conformer (NH···O=C), followed in energy ordering by the IIa_1 species (N···H−O).

Rotational Spectra

Initial surveys of the microwave spectrum were directed to the identification of the lowest energy conformers of Table 1, which are predicted to be near-prolate asymmetric tops. A search in a wide range around 8 GHz soon revealed a set of characteristic μ_a-type R-branch transitions. The optimal polarization conditions for these transitions were consistent with a relatively large μ_a electric dipole moment, as predicted for most of the type II (N···O−H intramolecular hydrogen bond) configurations of Table 1. These measurements, which led to the assignment of a first rotamer of the molecule, were later completed with other R-branch transitions with μ_b and μ_c selection rules. As exemplified in Figure 2, all measured transitions exhibited small hyperfine structures attributable to the nuclear quadrupole coupling interaction originated by a ^{14}N ($I = 1$) nucleus. This fact confirms that the spectrum was originated by a molecule containing a single nitrogen atom. The rotational frequencies were fitted to a Hamiltonian $H_R^{(A)} + H_Q$, where $H_R^{(A)}$ represents the Watson A-reduced semirigid rotor Hamiltonian[21] and H_Q represents the nuclear quadrupole coupling interaction term.[22,23] A satisfactory fit with residuals below

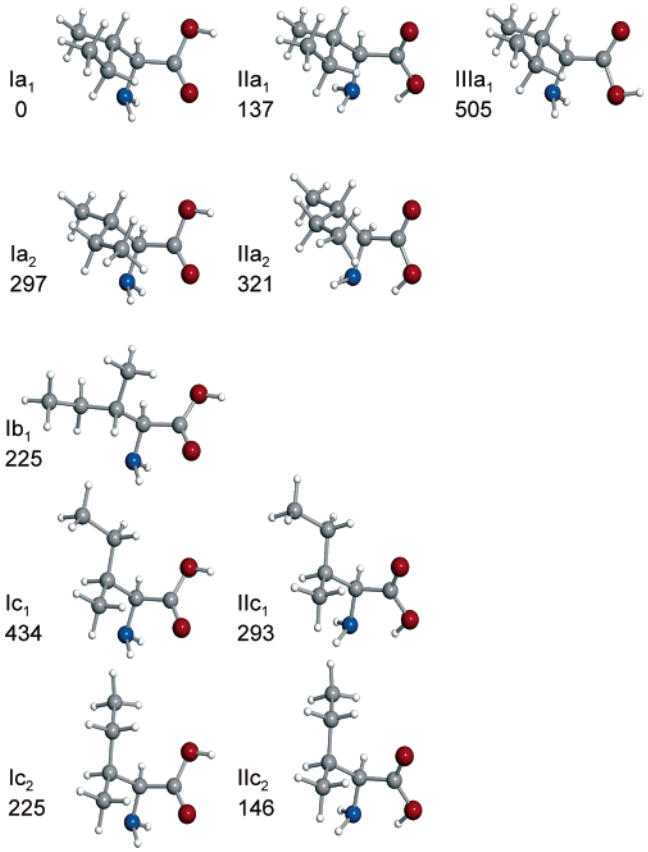

Figure 1. Geometries for the 10 lower energy structures calculated for isoleucine. Relative energies in wavenumbers.

frequency accuracy led to the spectroscopic parameters of Table 2. Examination of the experimental rotational constants revealed an excellent agreement with the predicted values for conformer IIa_1 in Table 1. A further confirmation of the identity of this conformer comes from the comparison between the experimental and predicted values for the ^{14}N nuclear quadrupole coupling constants χ_{aa}, χ_{bb}, and χ_{cc} (see Tables 1 and 2). These constants depend on the electronic environment around the amino nitrogen atom and are very sensitive to conformational changes, becoming a valuable identifier for the structure.[14−17] The excellent match of rotational constants and nuclear quadrupole coupling parameters specifically excluded the other type II conformers of Figure 1 which differ in the orientation of the side chain.

We pursued the search since a significant number of transitions, presumably belonging to other lower energy conformers of Figure 1, still remained unassigned in the spectrum. After a careful inspection, μ_c- and μ_b-type R-branch transitions of a second rotamer were assigned. The observation (Figure 2) of ^{14}N nuclear quadrupole coupling hyperfine structures positively confirmed a nitrogen-containing molecule. The non-observation of μ_a-type transitions suggested a weak or zero electric dipole moment component along this axis which is tenable for conformers of configuration I (N−H···O=C). Analysis of the rotational transitions followed the same method used for the previous conformer, yielding the rotational parameters shown in Table 2. The definitive proof to identify the new rotamer as conformer Ia_1 resulted again from the excellent agreement between the predicted and experimental rotational and nuclear quadrupole coupling constants listed in Tables 1 and 2. On this basis, all other lower energy type I conformers were excluded.

(20) Frisch, M. J. et al., *Gaussian 03*, revision B.04; Gaussian, Inc.: Wallingford, CT, 2004.
(21) Watson, J. K. In *Vibrational Spectra and Structure*; Durig, J. R., Ed.; Elsevier: Amsterdam, 1977; Vol. 6, pp 1−89.
(22) Gordy, W.; Cook, R. L. *Microwave Molecular Spectra*; Wiley: New York, 1984.
(23) Pickett, H. M. *J. Mol. Spectrosc.* **1991**, *148*, 371.

Table 1. Ab Initio (MP2/6-311++G(d,p)) Molecular Properties for the Ten Lower Energy Conformers of Isoleucine in Figure 1

	relative energies[a]		rotational constants			electric dipole moments[b]				nuclear quadrupole coupling constants		
conformers	ΔE/cm^{-1}	$\Delta(E+\mathrm{ZPE})$/cm^{-1}	A/MHz	B/MHz	C/MHz	μ_a/D	μ_b/D	μ_c/D	μ_T/D	χ_{aa}/MHz	χ_{bb}/MHz	χ_{cc}/MHz
Ia_1	9	0	2100	1106	980	0.3	0.5	1.0	1.2	−2.80	0.27	2.53
Ia_2	297	297	1959	1258	1127	0.2	0.2	1.1	1.2	−3.98	1.10	2.88
Ib_1	245	225	2677	987	847	0.5	0.7	0.9	1.2	−3.78	2.36	1.42
Ic_1	390	434	2137	1167	961	0.1	1.3	0.5	1.4	−0.45	−0.11	0.56
Ic_2	198	225	1851	1377	1085	0.6	1.3	0.1	1.4	0.30	−1.07	0.77
IIa_1	36	137	2192	1114	941	3.4	4.7	1.2	5.9	−3.32	2.03	1.29
IIa_2	160	321	2006	1266	1118	4.0	2.2	2.4	5.2	−3.85	1.87	1.98
IIc_1	174	293	2365	1113	959	1.5	4.5	1.9	5.1	0.25	2.58	−2.82
IIc_2	0	146	2023	1285	1084	1.2	4.2	2.6	5.1	−1.56	2.31	−0.75
$IIIa_1$	493	505	2121	1104	972	0.6	0.1	1.4	1.5	−2.41	−0.18	2.59

[a] Harmonic zero-point vibrational energy (ZPE) corrections calculated at B3LYP/6-311++G(d,p) level. [b] 1 D ≈ 3.3356 × 10^{-30} C m.

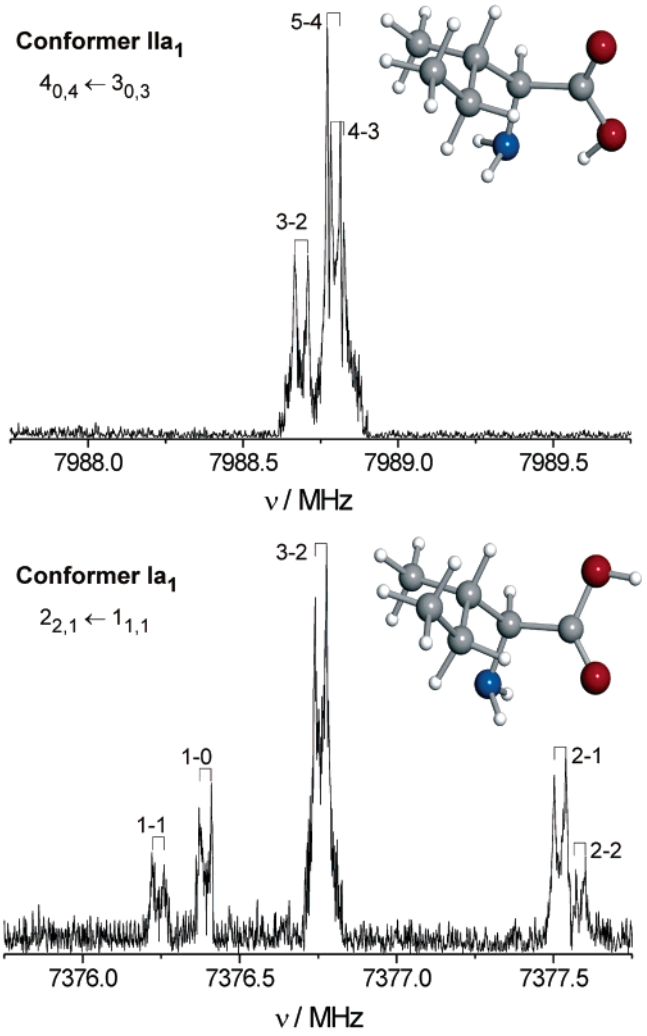

Figure 2. Rotational transitions $J_{K_{-1},K_{+1}} = 4_{0,4} \leftarrow 3_{0,3}$ (upper trace) and $2_{2,1} \leftarrow 1_{1,1}$ (lower trace) for the observed conformers IIa_1 and Ia_1, respectively, of neutral isoleucine in gas phase, split into several hyperfine components caused by the ^{14}N nuclear quadrupole coupling. Hyperfine components are labeled with quantum number $F = I + J$. Each component appears as a doublet due to the Doppler effect (see Experimental Methods).

Once the rotational transitions belonging to conformers IIa_1 and Ia_1 were measured, no transitions imputable to other conformers were left unassigned in the jet-cooled rotational spectrum. The experimental frequencies for the observed conformers are given as Supporting Information.

The relative populations of the observed conformers in the supersonic jet can be estimated from relative intensity measurements of the rotational transitions. If we admit that cooling in the adiabatic expansion brings all molecular species to their ground vibrational state,[15] the experimental intensities of lines for a conformer i are proportional to the corresponding electric dipole moment component μ_i and the number density of species i in the jet N_i. A comparison of experimental transition intensities between conformers Ia_1 and IIa_1 using a set of μ_c-type transitions, for which the predicted electric dipole moments are comparable, gave an approximate population ratio of $N(Ia_1)/N(IIa_1) = 2$. This postexpansion abundance qualitatively agrees with the hypothetical gas-phase equilibrium distribution calculated from the ab initio computations of Table 1, which predict conformer Ia_1 as the most stable of the molecule.

Table 2. Rotational Parameters of Isoleucine

	conformer IIa_1	conformer Ia_1
A/MHz[a]	2186.32958(62)[f]	2089.11492(40)
B/MHz	1113.48042(15)	1109.60237(91)
C/MHz	932.49877(14)	973.55058(65)
Δ_J/kHz[b]	0.2255(22)	0.1423(103)
Δ_{JK}/kHz	−0.807(13)	[0.0][g]
Δ_K/kHz	1.62(13)	0.586(39)
δ_J/kHz	0.04043(102)	0.1022(95)
δ_K/kHz	0.617(41)	0.95(31)
χ_{aa}/MHz[c]	−3.4431(53)	−2.5609(68)
χ_{bb}/MHz	1.9378(26)	0.2030(22)
χ_{cc}/MHz	1.5053(26)	2.3579(22)
σ/kHz[d]	1.7	1.9
N[e]	83	38

[a] A, B, C represent the rotational constants. [b] Δ_J, Δ_{JK}, Δ_K, δ_J, δ_K are the quartic centrifugal distortion constants. [c] $\chi_{\alpha\beta}$ ($\alpha,\beta = a$, b, or c) are ^{14}N nuclear quadrupole coupling parameters. [d] rms deviation of the fit. [e] Number of fitted transitions. [f] Standard error in parentheses in units of the last digit. [g] Parameters in square brackets were kept fixed in the fit.

Discussion

Two conformers of neutral isoleucine have been observed in a supersonic jet expansion of the laser vaporized compound. The results presented in this work constitute an important piece of information to complete the conformational landscape of aliphatic α-amino acids. The comparison of the conformations observed in isoleucine with the other three hydrophobic natural amino acids (glycine,[8,9] alanine,[10,15] valine[16]) studied to date in gas phase reveals consistent regularities. In all cases, the global minimum of the molecule is associated with the type I arrangement (glycine I, alanine I, valine Ia, isoleucine Ia_1). This configuration benefits not only from the nearly bifurcated intramolecular hydrogen bond N−H···O═C, but also from a cis arrangement of the carboxylic group. Theoretical predic-

tions[24] claim that the stabilization contribution of the N···H−O interaction, observed in the second most stable conformers of the four aliphatic amino acids (glycine II, alanine IIa, valine IIa, isoleucine IIa_1), is nearly twice that of the N−H···O═C. However, the type II configuration requires a trans arrangement for the carboxylic group, imposing a considerable energy penalty[25] that counterbalances the total relative energies.

The relatively large size of the *sec*-butyl side chain of isoleucine can give rise to multiple conformers. However, the parallelisms in the arrangement finally adopted in gas phase by the side chains of isoleucine and valine[16] are also noticeable. The side chain adopts the same configuration in the two observed conformers of each molecule, reflecting small interactions between the apolar side chains and the amino acid skeleton. Moreover, the relative orientation of the substituents at C_β is similar in isoleucine and valine, adopting the same staggered arrangement denoted "a" ($\angle(H_\alpha-C_\alpha-C_\beta-H_\beta) \approx 60°$) in Chart 3, which in the conventional view presumably minimizes the steric repulsion in both molecules. In isoleucine the terminal methyl group adopts a trans orientation ($\angle(C_\alpha-C_\beta-C_\gamma-C_\delta) \approx 180°$) with respect to C_α, which moves away the methyl group from the amino acid skeleton and is comparable to the lowest energy trans configuration of small alkanes.[26]

As observed in other experiments conducted in supersonic expansions, the number of observed conformers in the jet-cooled spectrum is very small compared to the number of thermically accessible conformers corresponding to the equilibrium distribution predicted ab initio. This fact can be explained in terms of collisional relaxation in the expansion. In this process local minima may collapse to the preferred lower energy conformers if they are separated by affordable barriers,[27,28] and therefore the total number of finally observed species is generally small. Conformer interconversion is enhanced using heavier carrier gases, as evidenced in hydrogen-bonded complexes.[29] The inability to observe a plausible configuration III in glycine, alanine, valine, and isoleucine in a supersonic jet can be attributed to relaxation to configuration I. This argument is supported with the relatively small III → I interconversion barriers determined for glycine and alanine.[15,27] A similar argument could be invoked to justify that only one conformation is observed for the side chain orientation in isoleucine and valine.

The comparative study of the conformational landscape of all the aliphatic natural amino acids will be completed with future conformational studies of larger amino acids. The present work is further evidence of the relevant contribution of laser-ablation molecular-beam Fourier transform microwave spectroscopy to the structural investigation of isolated biomolecules.

Acknowledgment. We would like to thank the DGI − Ministerio de Ciencia y Tecnología (project BQU2003-03275) for financial support.

Supporting Information Available: Tables of experimental rotational frequencies of the observed conformers of isoleucine and complete ref 20. This material is available free of charge via the Internet at http://pubs.acs.org.

JA0528073

(24) (a) Hu, C. H.; Shen, M.; Schaefer, H. F., III. *J. Am. Chem. Soc.* **1993**, *115*, 2923. (b) Gronert, S.; O'Hair, R. A. J. *J. Am. Chem. Soc.* **1995**, *117*, 2071. (c) Császár, A. *J. Phys. Chem.* **1996**, *100*, 3541.
(25) Császár, A.; Allen, W. D.; Schaefer; H. F., III. *J. Chem. Phys*. **1998**, *108*, 9751.
(26) (a) Bartell, L. S.; Kohl, D. A. *J. Chem. Phys*. **1963**, 39, 3097. (b) Smith, G. D.; Jaffe, R. L. *J. Phys. Chem.* **1996**, *100*, 18718.
(27) (a) Ruoff, R. S.; Klots, T. D.; Emilsson, T.; Gutowsky, H. S. *J. Chem. Phys*. **1990**, *93*, 3142. (b) Godfrey, P. D.; Brown, R. D.; Rodgers, F. M. *J. Mol. Struct.* **1996**, *376*, 65.
(28) (a) Florio, G. M.; Christie, R. A.; Jordan, K. D.; Zwier, T. S. *J. Am. Chem. Soc.* **2002**, *124*, 10236. (b) Godfrey, P. D.; Brown, R. D. *J. Am. Chem. Soc.* **1998**, *120*, 10724.
(29) (a) Antolínez, S.; López, J. C.; Alonso, J. L. *Angew. Chem., Int. Ed.* **1999**, *38*, 1772. (b) Antolínez, S.; López, J. C.; Alonso, J. L. *Chem. Phys. Chem.* **2001**, *2*, 114. (c) Sanz, M. E.; Lesarri, A.; López, J. C.; Alonso, J. L. *Angew. Chem., Int. Ed.* **2001**, *40*, 935. (d) Sanz, M. E.; Lopez, J. C.; Alonso, J. L. *Chem.−Eur. J.* **2002**, *8*, 4265.